3D Ultrasound Transmission Tomography Using Synthetic Aperture Focusing and Regularized Algebraic Reconstruction

[1]R. Jiřík, [1]I. Peterlík, [1]J. Jan, [1]J. Fousek, [2]M. Zapf, [2]N. Ruiter

[1] Dept. of Biomedical Engineering, Brno University of Technology, Czech Republic,
[2] Karlsruhe Institute of Technology, Germany
Email: jirik@feec.vutbr.cz

Abstract. *Ultrasound transmission tomography is presented as an imaging modality for breast cancer diagnosis. A 3D reconstruction technique is proposed for estimation of sound-speed images for the Karlsruhe 3D ultrasound transmission tomograph. The problems of sparse spatial distribution of ultrasound transducers and of low signal-to-noise ratio are approached using synthetic aperture focusing. The image reconstruction is done based on regularized algebraic reconstruction. The proposed method is tested on simulated data as well as on measured phantom data.*

Keywords: ultrasound transmission tomography, sound speed, synthetic-aperture focusing, regularization

1. Introduction

Ultrasound computed tomography (USCT) is an imaging modality intended as an alternative to X-ray and conventional ultrasound imaging for breast cancer diagnostics. The acquisition setup is similar to X-ray computed tomography (CT) [1]. The imaged object is immersed in a water tank, surrounded by ultrasound transducers, where one transducer emits ultrasound wave while other transducers receive the transmitted and reflected/scattered signals. Images of several diagnostically important parameters can be reconstructed from the received signals: reflectivity, sound-speed and attenuation. This contribution focuses on sound-speed image reconstruction.

The USCT systems are still in the stage of research, mainly due to the complexity caused by phenomena inherent to ultrasound signal propagation, such as diffraction and refraction. Most published USCT devices are constructed as 2D systems (e.g. [2]), with a ring of fairly large transducers. Our approach is based on the Karlsruhe 3D USCT system, described in [3], where transducers are positioned on the surface of a cylindrical tank. Such transducer distribution enables fast acquisition of spatial 3D data and potentially a better spatial resolution of reflectivity images. However, it brings also several challenges, mainly sparse transducer distribution and low signal-to-noise ratio (SNR) due to small transducer size.

An approach to overcome the sparse transducer distribution and low SNR by means of synthetic-aperture focusing is presented. Example results reconstructed from synthetic data and data measured on a breast phantom are shown.

2. Subject and Methods

The problem of 3D sound-speed image reconstruction can be formulated as reconstruction from projections. Here, the projections are formed by time-of-flight (TOF) values, i.e. the ultrasound propagation times measured for each emitter-receiver combination. The sound-speed image reconstruction is solved as a 3D regularized algebraic reconstruction [4]. In contrast to the widely used filtered backprojection method, the algebraic reconstruction enables regularization of the reconstruction. Here, the regularization imposes piecewise smoothness of the resulting sound-speed map, while preserving edges (details can be found in [4]). In addition, the algebraic reconstruction approach enables incorporation of non-straight propagation paths, e.g. due to refraction (not implemented here).

The data acquisition is done in 6 steps. After each step the whole USCT system is rotated, in order to increase the number of effective transducer positions [3]. Hence, the system has 6 times more "virtual transducer positions" than the physical number of transducers. The received radiofrequency transmission signals are measured and stored for all emitter-receiver combinations within each rotation position. This allows us to use a synthetic aperture formed of nearby virtual transducer positions by appropriately delaying and summing their radiofrequency signals. The aperture size is given by the number of neighbouring transducers used for focusing.

The focusing procedure is done in two steps: first, focusing on the receiver side (delay and sum of the radiofrequency signals) is done with the focal point positioned to each emitter of the emitter aperture. Then, the resulting focused signals are focused (i.e. accordingly delayed) so that the emitter aperture is focused to the center of the receiver aperture.

As it is practically impossible to run the above described processing on a standard PC computer (a dataset consists of about 3.5 million radiofrequency signals, which needs approximately 20 GB of storage capacity), the algorithm was parallelized and implemented using Matlab® Parallel Computing Toolbox™ and Matlab® Distributed Computing Server™ in a heterogeneous computing cluster environment.

3. Results

Simulated data

The sound-speed reconstruction was first tested on synthetic data. The simulation software was implemented to mimic the Karlsruhe 3D USCT system in the geometry and the data acquisition scheme. The radiofrequency signals were generated assuming propagation of spherical waves, with the centre frequency of 3 MHz and a bandwitdh of 1.2 MHz. Frequency-independent attenuation along the propagation path was implemented. The propagation path between each emitter and receiver was assumed straight, i.e. no refraction was simulated. The resulting synthetic radiofrequency signals were distorted by additive Gaussian white noise. The signal-to-noise was set to 11 dB, which corresponds to the ratio estimated from the data measured using the Karlsruhe 3D USCT system. The simulated object was a simple model of breast immersed in water. It consisted of several homogeneous regions with different ultrasound speed values. The hemisphere simulating a breast shape included three spherical objects simulating various lesions. The simulated sound-speed values corresponded to the expected values for breast tissues [5] (1493 m/s for normal breast tissue, 1550 m/s for breast cancer lesion, 1568 m/s for cyst and 1584 m/s for fibroadenoma). The attenuation coefficient for the breast tissues was 0.7 dB/cm/MHz and for water regions it was set to 0 dB/cm/MHz.

The accuracy of the estimated sound-speed maps for various focusing apertures was evaluated in terms of the mean squared difference between the estimated map and the reference sound-speed map used for synthetic-data generation. The error values for some synthetic apertures are shown in Table 1 (note that the spacing between emitter and receiver elements are different). They show that too small and too large aperture size deteriorate the image quality. An optimal size of the emitting and receiving apertures has to be selected as a compromise between a too small aperture (influence on noise) and a too large aperture (geometry distortion due to loss of spatial information).

Table 1. Mean square errors of sound-speed maps for simulated USCT data, various combinations of the synthetic aperture sizes.

Emitting and receiving apertures [no. of virtual transducer positions]	Emitting and receiving apertures [mm x mm]	Mean square error [$(m/s)^2$]
1 x 1, 1 x 1	1 x 1, 1 x 1	72
3 x 3, 7 x 7	12 x 12, 18 x 18	54
7 x 7, 13 x 13	24 x 24, 36 x 36	79

Measured phantom data

The sound-speed reconstruction with synthetic-aperture focusing described above was tested on data recorded with the Karlsruhe 3D USCT system on a breast phantom with embedded cyst-mimicking lesions (CIRS triple modality breast phantom). To evaluate visually the sound-speed maps based on known outlines of structures in the selected slice, a reflectivity image was reconstructed using an algorithm described in [3] (Fig. 1 a, b). The breast-phantom outlines are denoted by dotted lines. Sound-speed maps in the selected slices are shown for the optimal aperture sizes in Fig. 1 c, d. Examples of images obtained for no focusing and too large synthetic apertures are shown in Fig. 2. The images show that optimal focusing substantially improves the spatial consistence over no focusing (which lacks spatial consistence) and over too large aperture used for focusing (which leads to blurred images). The sound-speed of the main-body material was in accordance with the phantom specifications (approximately 1450 m/s).

The reconstructed 3D images showed clear outlines of the breast phantom. However the phantom geometry was slightly deformed. The breast object appeared smaller than in the reflectivity images. The lesions from the reflectivity images were visible also in the sound-speed image (consistently in neighboring layers) but in shifted positions. This can be explained by beam refraction. Due to the cone-like shape of the breast phantom, for some emitter-receiver combinations the ultrasound beam path is close to a tangent to the breast surface. The refraction effect is not taken into account by the presented image reconstruction because it assumes straight beams.

4. Discussion and Conclusions

The presented synthetic-aperture focusing improves the reconstruction of sound-speed images in case of sparse distribution of small transducers in USCT. The synthetic aperture size has to be chosen as a compromise. Larger aperture leads on one hand to better suppression of diffraction and higher SNR, while, on the other hand, decreasing the spatial resolution of the reconstructed images.

To account for beam refraction, this effect will be included in the algebraic reconstruction algorithm by assuming non-straight beam-propagation path. The evaluation will be extended by construction and imaging of a sound-speed phantom with completely known reference sound-speed values for all used materials.

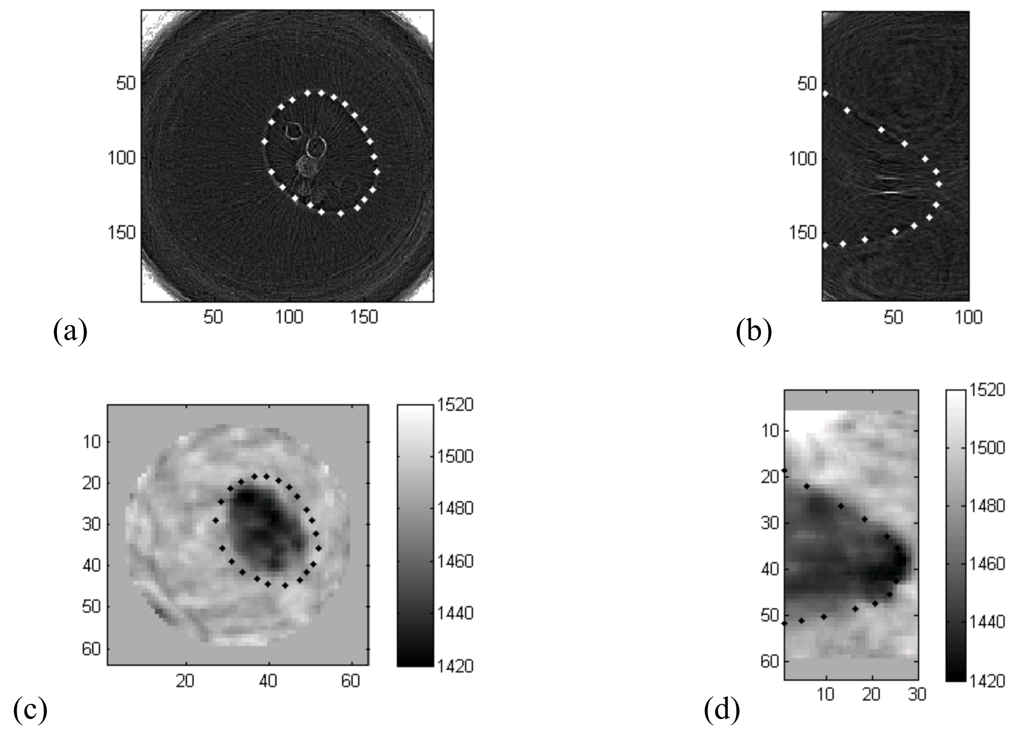

Fig. 1. (a), (b) Reflectivity images, coronal and sagittal slices, respectively. (c), (d) Sound-speed images, coronal and sagittal slices, respectively, optimal synthetic aperture size (12x12, 18x18 mm for emitter and receiver apertures).

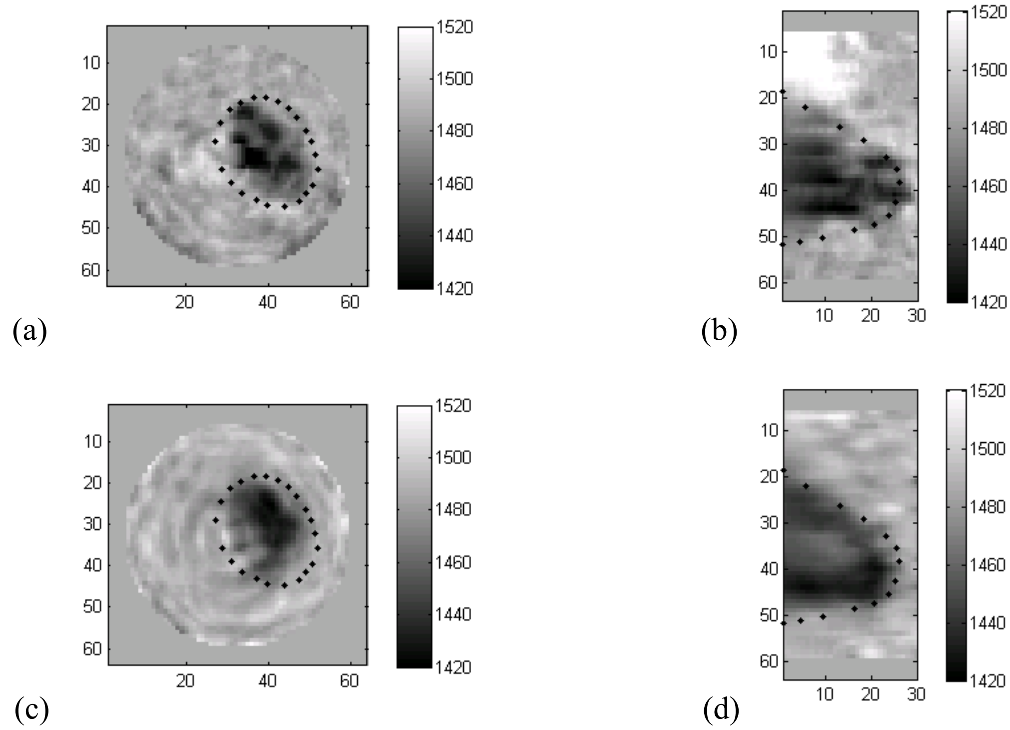

Fig. 2. (a), (b) Sound-speed images, coronal and sagittal slices, respectively, no focusing. (c), (d) Sound-speed images, coronal and sagittal slices, respectively, too large synthetic aperture size (24x24, 36x36 mm for emitter and receiver apertures).

Acknowledgements

The project has been supported by the Czech Ministry of Education, Youth and Sports (Research Center DAR, proj. no. 1M6798555601) and the joint program of the German Academic Exchange Service and the Czech Academy of Science, partly also by the research frame of the Czech Ministry of Education, Youth and Sports (grant no. CEZ MS 0021630513). We are also grateful to MetaCentrum, an activity of the CESNET association, for offering the distributed-computing resources.

References

[1] Kak AC, Slaney M. Principles of Computerized Tomographic Imaging. Society of Industrial and Applied Mathematics; 2001.

[2] Duric N, Littrup P, Poulo L, Babkin A, Pevzner R, Holsapple E, Rama O, Glide C. Detection of breast cancer with ultrasound tomography: First results with the Computed Ultrasound Risk Evaluation (CURE) prototype. Med Phys 2007;34:773–785.

[3] Gemmeke H, Ruiter NV. 3D Ultrasound Computer Tomography for Medical Imaging. Nuclear Instruments and Methods in Physics Research. 2007; 550:1057–1065.

[4] Jiřík R, Peterlík I, Jan J, Ruiter NV, Zapf M. 3D Regularized Speed-Map Reconstruction in Ultrasound Transmission Tomography. 2009 IEEE International Ultrasonics Symposium, Roma, Sept. 2009. 2272–2275.

[5] Glover GH, Sharp JC. Reconstruction of ultrasound propagation speed distribution in soft tissue: Time-of-flight tomography. IEEE Trans. Sonic and Ultrasonics 1977; 24:229–234.